Alteration of Cx43:Cx40 expression ratio in A7r5 cells

Janis M. Burt, Anna M. Fletcher, Timothy D. Steele, Yan Wu, G. Trevor Cottrell and David T. Kurjiaka

---

You might find this additional information useful...

This article cites 34 articles, 24 of which you can access free at:
http://ajpcell.physiology.org/cgi/content/full/280/3/C500#BIBL

This article has been cited by 4 other HighWire hosted articles:

Connexin expression and conducted vasodilation along arteriolar endothelium in mouse skeletal muscle
R. C. Looft-Wilson, G. W. Payne and S. S. Segal
J Appl Physiol, September 1, 2004; 97 (3): 1152-1158.
[Abstract] [Full Text] [PDF]

Sharing signals: connecting lung epithelial cells with gap junction channels
M. Koval
Am J Physiol Lung Cell Mol Physiol, November 1, 2002; 283 (5): L875-L893.
[Abstract] [Full Text] [PDF]

Cx40 and Cx43 expression ratio influences heteromeric/ heterotypic gap junction channel properties
G. T. Cottrell, Y. Wu and J. M. Burt
Am J Physiol Cell Physiol, June 1, 2002; 282 (6): C1469-C1482.
[Abstract] [Full Text] [PDF]

Heterotypic gap junction channel formation between heteromeric and homomeric Cx40 and Cx43 connexons
G. T. Cottrell and J. M. Burt
Am J Physiol Cell Physiol, November 1, 2001; 281 (5): C1559-C1567.
[Abstract] [Full Text] [PDF]

Medline items on this article's topics can be found at http://highwire.stanford.edu/lists/artbytopic.dtl
on the following topics:
Oncology .. Gap Junctions
Biochemistry .. Antisense DNA
Oncology .. Protein Expression
Endocrinology .. Connexins
Developmental Biology .. Aging

Updated information and services including high-resolution figures, can be found at:
http://ajpcell.physiology.org/cgi/content/full/280/3/C500

Additional material and information about *AJP - Cell Physiology* can be found at:
http://www.the-aps.org/publications/ajpcell

This information is current as of September 10, 2008 .

Alteration of Cx43:Cx40 expression ratio in A7r5 cells

JANIS M. BURT, ANNA M. FLETCHER, TIMOTHY D. STEELE,
YAN WU, G. TREVOR COTTRELL, AND DAVID T. KURJIAKA
Department of Physiology, University of Arizona, Tucson, Arizona 85724

Burt, Janis M., Anna M. Fletcher, Timothy D. Steele, Yan Wu, G. Trevor Cottrell, and David T. Kurjiaka.
Alteration of Cx43:Cx40 expression ratio in A7r5 cells. *Am J Physiol Cell Physiol* 280: C500–C508, 2001.—Connexins (Cx) 40 and 43 are coexpressed by several cell types at ratios that vary as a function of development, aging, and disease. Because these connexins form heteromeric channels, changes in expression ratio might be expected to significantly alter the connexin composition of the gap junction channel population and, therefore, gap junction function. To examine this possibility, we stably transfected A7r5 cells, which naturally coexpress Cx43 and Cx40, with a vector encoding antisense Cx43. Cx43 mRNA continued to be expressed in the antisense transfected clones, although levels were inversely related to the number of copies of antisense DNA incorporated into the genome. Protein levels, quantified in the clones with the highest and lowest Cx43:Cx40 mRNA ratios, were not well predicted by the mRNA levels, although the trends predicted by the Cx43:Cx40 mRNA ratio were preserved. Electrical coupling did not differ significantly between clones, but the clone with elevated Cx43:Cx40 protein expression ratio and unchanged Cx43 banding pattern was significantly better dye coupled than the parental A7r5 cells. These results suggest that as the Cx43:Cx40 ratio increases, provided alterations of Cx43 banding pattern (phosphorylation) have not occurred, permeability to large molecules increases even though electrical coupling remains nearly constant.

gap junctions; connexin40; connexin43; heteromeric channel; antisense

GAP JUNCTIONS are clusters of channels that connect cytosols of neighboring cells such that small molecules can readily diffuse between cells (for review, see Ref. 6). Two hemichannels (connexons) comprise a functional channel. Six subunits, called connexins, comprise each connexon. To date, 15 connexins have been identified in the mammalian genome. They are distinguished from one another by their predicted molecular masses in kilodaltons, with connexin43 (Cx43) and 40 (Cx40) representing connexins of 43 and 40 kDa, respectively. When all 12 connexins comprising the functional channel are identical, the channel is referred to as homomeric/homotypic. In their homomeric/homotypic forms, the various connexins exhibit unique functional properties such as phosphorylation- and voltage-dependent gating and permselectivity.

Many cells express more than one connexin, some of which can combine to form functional heteromeric and heterotypic channels. When the connexins comprising a connexon are not identical, the connexon is heteromeric. When the connexin composition of the two connexons comprising a channel differ, the channel is heterotypic. Despite the failure of Cx40 and Cx43 to form functional homomeric/heterotypic channels in the *Xenopus* oocyte expression system (36), Cx40 and Cx43 form such channels in mammalian cells (Cottrell GT and Burt JM, unpublished observations) (31). In addition, these connexins form heteromeric channels (17), and recent evidence suggests that they form functional heteromeric/heterotypic channels (Cottrell GT and Burt JM, unpublished observations) (16). Available data indicate that these mixed channels display unique conductance and gating properties.

Vascular smooth muscle cells express Cx43 and Cx40 to varying degrees (2, 3, 8, 9, 22, 25, 29). The homomeric/homotypic channels formed by Cx43 and Cx40 exhibit unique *1*) unitary conductances (1, 7, 26, 34, 35), *2*) voltage-dependent gating properties (4, 5, 7), and *3*) permeability characteristics (1, 7, 12, 34, 35). Focusing on the latter, Cx43 channels permit free exchange between cells of both anionic and cationic molecules of significant size. In contrast, Cx40 channels appear to mediate the exchange of cations far more readily than anions (see, however, Ref. 12) and of small molecules far more readily than large molecules. As a result, the functional ramifications of heteromeric Cx43–40 channel formation could be profound. For example, heteromeric channels of Cx40 and Cx43 exhibit a broad array of unitary conductances defined at either end by the conductances of the homomeric/homotypic channels (17). It is likely that this array of conductances is indicative of a broad array of permeability properties. Cx43–40 heteromeric channels also exhibit voltage-dependent gating properties distinct from either the Cx43 or Cx40 homomeric/homotypic channels. Given the differences in phosphorylation-dependent gating behavior of homomeric/homotypic Cx43 vs. Cx40 channels, it is likely that heteromeric channels will display a range of sensitivity to the pathways involved in acute regulation of cell processes. Thus cells that form heteromeric channels may be able

---

http://www.ajpcell.org

to adjust their communication properties over a broad physiological range acutely through phosphorylation-dependent mechanisms and over a longer time frame by regulating the ratio of expressed connexins.

The goal of the current study was to develop smooth muscle cell lines that would facilitate exploration of the ramifications of coexpression of Cx40 and Cx43 at varying ratios. Toward this end, we stably transfected A7r5 cells, from a vascular smooth muscle cell line in which Cx40 and Cx43 are naturally coexpressed (23, 24), with a vector encoding antisense Cx43 (Cx43AS). Clones of these cells as well as cells of the parental population were isolated, and mRNA and protein levels were determined. The communication properties of those clones with the most extreme Cx43:Cx40 protein ratios were determined. A clone with elevated Cx43:Cx40 protein ratio wherein Cx43 phosphorylation was unchanged displayed significantly enhanced dye coupling despite comparable levels of electrical coupling, suggesting that by controlling the expression ratio of these proteins, the cells directly regulate the types of communicated molecules. A clone with elevated Cx43:Cx40 protein ratio with significant amounts of Cx43 phosphorylation failed to show increased communication levels, suggesting that cells can regulate the communication pathway through signaling cascades as well. These cell lines should prove useful in understanding the rules of heteromeric channel assembly and the physiological significance of heteromerization to intercellular communication and cell function.

MATERIALS AND METHODS

Vectors. A7r5 cells were transfected with pRSV-Cx43AS, pCMV-Cx43AS [obtained from Dr. Alan Lau (15)], or pRc/CMV (Invitrogen, San Diego, CA). The pRSV vector was made by excising full-length Cx43 from clone G2B (courtesy of Dr. Eric Beyer) with the restriction enzyme *Eco*RI and then subcloning the excised fragment into the unique *Sal*I cloning site of pRXneo (obtained from Dr. Roger Miesfeld) by using a blunt-end ligation strategy.

Transfection and cell culture. A7r5 cells were transfected after subculture and growth to 50–75% confluence level in 60-mm plates. Cells were exposed to pRSV-Cx43AS, pCMV-Cx43AS, or pRc/CMV vector DNA as a calcium phosphate/DNA precipitate (Profection; Promega) according to the manufacturer's instructions. Neomycin-resistant cells were selected at 250 μg/ml G418 (GIBCO BRL). At confluence, they were dilution cloned. Cells were maintained, after their expansion from single-cell clones, in DMEM (GIBCO) supplemented with 10% fetal bovine serum (FBS) and antibiotics (3% penicillin, 5% streptomycin) at 37°C and 5% CO_2. For transfectants, culture medium also contained 250 μg/ml G418.

RNA isolation, detection, and quantification. Preliminary screening of total RNA by standard Northern techniques suggested that Cx43 was elevated in cells that had been transfected with the Cx43 antisense vector. Because only mRNA that successfully exits the nucleus can be translated, we determined the Cx43 and Cx40 mRNA content of the cytoplasmic fraction of total RNA. Cytoplasmic RNA was isolated as follows. Confluent cells (maintained in 10% FBS) were washed with PBS, aspirated "dry," and lysed (0.65% Nonidet P-40, 0.15 M NaCl, 0.01 M Tris·HCl, and 0.0015 M

$MgCl_2$, pH 7.4) such that nuclei remained intact and stuck to the dish. The lysate was collected and centrifuged to remove cellular debris. Urea buffer (7 M urea, 0.35 M NaCl, 0.01 M Tris·HCl, 0.01 M EDTA, and 1% SDS, pH 7.4) was added to the lysate, and the mixture was phenol extracted twice and chloroform extracted once. RNA was then precipitated in ethanol, pelleted, and dried.

Cytoplasmic RNA was denatured and slotted onto Zeta-Probe GT membrane (Bio-Rad), in duplicate, at 10 μg/sample. The duplicate blots were probed for connexin mRNAs with the use of end-labeled (30) 48-mer oligomers or random primer-labeled cDNAs. The Cx40 48-mer was complementary to bases 876–923 in the coding sequence of rCx40; the Cx43 48-mer was complementary to bases 714–762 in the coding sequence of rCx43. Random primer-labeled cDNA probes (Prime-a-gene Kit from Promega, used according to the manufacturer's instructions) were made by using a 591-bp fragment of the rCx40 sequence or a 1393-bp fragment of rCx43. Sample comparisons were made after the connexin content of a sample was normalized to its glyceraldehyde-3-phosphate dehydrogenase (GAPDH) content, which was detected by using random primer-labeled GAPDH made from a 770-bp fragment of the hGAPDH sequence. For both types of probes, hybridizations and washes were done in standard sodium phosphate solutions at 65°C overnight (ZetaProbe GT manual) or in Quickhyb (Stratagene) at 68°C for 1–2 h with comparable results. Radioactivity was visualized via PhosphorImager (Molecular Dynamics), and sample intensity was assessed using the software provided by the manufacturer.

Sample intensity was converted to micrograms of bound cDNA probe or micromoles of oligomer probe as follows. The specific activity (cpm/μg or cpm/μmol) of each probe was calculated after trichloroacetic acid (TCA) precipitation. A membrane strip spotted with 10^5, 10^4, 10^3, 10^2, and 10^1 cpm (determined by scintillation counting) of the probe used to hybridize each blot was imaged simultaneously with each blot. The screen intensity of each spot was plotted as a function of the spotted counts per minute to verify the linear range of detection and to establish the relationship between image intensity and probe counts per minute. Counts per minute hybridized to each sample could then be calculated, and the micrograms (cDNA probe) or micromoles (oligo probe) of connexin could be calculated from the specific activity of the probe. With the cDNA probes, Cx43 was 2.357 times more likely to be detected than Cx40 because of the differing lengths of the template DNA (1393/591). Consequently, comparisons of Cx40 and Cx43 contents from cDNA probes were made after the Cx40 results were multiplied by 2.357. This correction was not used for the data derived from end-labeled oligomer probe, wherein each copy of mRNA should hybridize with only one copy of probe.

Modified Southern analysis. To estimate the number of copies of the antisense Cx43 sequence stably incorporated into the genome, we screened our transfectants for the amount of RSV (Rous sarcoma virus) promoter sequence in the DNA as follows. Cells were pelleted and subsequently lysed by heating at 100°C for 10 min in a solution containing 0.4 M NaOH and 10 mM EDTA, and cells were then slotted onto nylon membrane (Zeta-Probe GT). The blot was hybridized with an RSV cDNA random primer-labeled probe, which was made by using an ~320-bp fragment of RSV that was released from pRXneo after digestion with restriction enzymes *Hinf*I and *Hind*III and then gel purified. RSV content was visualized and quantified as described in *RNA isolation, detection, and quantification.* After image analysis was completed, the blot was stripped and probed with random primer-labeled GAPDH cDNA. The relative RSV content of
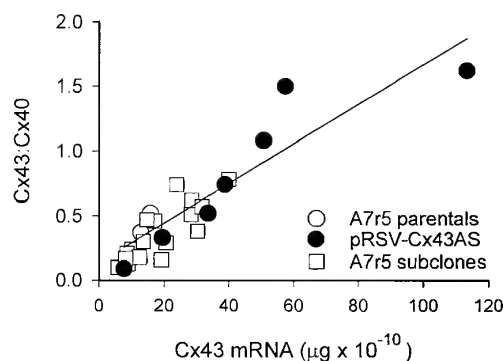
Fig. 1. Cx43:Cx40 mRNA ratio vs. Cx43 mRNA content of A7r5 cells and clones. Data were determined from cytoplasmic RNA probed with end-labeled oligomer. Note the broad range of values for Cx43 and the Cx43:Cx40 ratio. The ratio was linearly related to Cx43 content ($r^2 = 0.82$, $P < 0.05$). Cx, connexin; RSV, Rous sarcoma virus; Cx43AS, antisense Cx43 clone.

Table 1. *Cx43 and Cx40 mRNA and protein contents and Cx43:Cx40 ratios of A7r5 parental cells and several A7r5 cell clones*

Clone	Cx43 mRNA,[a] µg	Cx40 mRNA,[a] µg	Cx43/Cx40	Clone Ratio/ Parental Ratio
6B5N	297	184	1.6	4.7
2A6	20.5	224	0.09	0.26
A7r5[c]	34 ± 11	117 ± 49	0.34	

Clone	Cx43 mRNA,[b] pmol	Cx40 mRNA,[b] pmol	Cx43/Cx40	Clone Ratio/ Parental Ratio
6B5N	14.9	5.9	2.6	4.2
2A6	2.8	8.1	0.35	0.56
A7r5[c]	3.8 ± 0.7	6 ± 1	0.62	

Clone	Cx43 protein,[d] fmol	Cx40 protein,[e] fmol	Cx43/Cx40	Clone Ratio/ Parental Ratio
6B5N	22 ± 1.3[g]	32 ± 1.8[f]	0.67	1.81
2A6	15 ± 0.5[f]	74 ± 4.7[f]	0.20	0.54
CMV23	41 ± 3.1[f]	46 ± 2.5[f]	0.88	2.38
A7r5	22 ± 0.9[g]	59 ± 5.9[f]	0.37	

Cx, connexin. [a]Determined with cDNA probe; [b]determined with oligomer probe. [c]Data represent means ± SE of 3 samples; [d]data represent means ± SE of 4 sample sets; [e]data represent means ± SE of 3 sample sets. [f]Different at $P \ll 0.05$ from all other clones (ANOVA, Tukey's post hoc comparison). [g]Different from all but 6B5N or A7r5 (ANOVA, Tukey's post hoc comparison).

each clone was determined after the RSV data were normalized to the GAPDH data.

Detection of Cx43 antisense mRNA. The antisense mRNA could not be detected in any of the antisense-transfected clones by using the procedures described for detection of mRNA. To increase our chances of detecting the antisense mRNA, we developed a ribonuclease protection assay (RPA). Total RNA (10 µg) and riboprobe were hybrized overnight at 42°C and treated with RNase A/RNase T1 (Ambion RPA kit), and probe/RNA complexes were visualized on an Instant Imager (Packard Instruments) after electrophoretic separation on 8 M urea, 4% polyacrylamide gels. Riboprobes were transcribed (using Promega's Riboprobe transcription systems according to manufacturer's recommendations) from linearized vector from the SP6 or T7 promoters. The Cx43AS probe was 541 nucleotides in length, 483 of which were complementary to bases 1–483 of the antisense sequence. Cx43 sense mRNA, Cx40, and GAPDH were also detected. The Cx43 probe was 315 nucleotides in length, 233 of which were complementary to bases 915–1148 of the Cx43 sequence. The Cx40 probe was 497 nucleotides in length, 447 of which were complementary to bases 597–1039 of the Cx40 sequence. The GAPDH probe (transcribed from pTRI-GAPDH-Rat from Ambion) was 383 nucleotides in length, 316 of which complemented the 3′ terminus of the coding sequence. Specific activity for all probes was determined after TCA precipitation.

Western analysis. Total protein was isolated from 100-mm dishes of confluent cells by using standard procedures and was then quantified (Pierce BCA Protein Assay Kit). Proteins were electrophoretically separated on 10% SDS gels, electrophoretically transferred to nitrocellulose (Hybond ECL, Amersham Pharmacia Biotech), and blocked with 5% nonfat dry milk (NFDM) in Tris-buffered saline supplemented with 0.5% Tween 20 (TTBS) (30). Blots were incubated overnight at 4°C with primary antibody, polyclonal affinity-purified Cx43 (Sigma), or Cx40 (Dr. Alex Simon) diluted 1:4,000 in 1% NFDM-TTBS. After several washes, blots were incubated with either horseradish peroxidase (HRP)-conjugated antirabbit Ig (diluted 1:5,000; Amersham Pharmacia Biotech) or ^{35}S-labeled anti-rabbit Ig (0.4 µCi/ml; Amersham Pharmacia Biotech). HRP signal was detected with the use of enhanced chemiluminescence (ECL; Pierce SuperSignal) and X-ray film. Connexin expression levels were quantified from blots probed with ^{35}S-labeled secondary antibody, which was visu-

alized in a position-specific manner with the use of an Instant Imager (Packard Instruments). For quantification, each gel was loaded with several samples, protein ladder, and either Cx40 or Cx43 standards. Standards were prepared by using glutathione S-transferase (GST)-fusion protein constructs of the COOH termini of Cx43 and Cx40 (provided by Drs. Alan Lau and David Paul, respectively). GST-fusion proteins were purified directly from bacterial (BL21) lysates with the affinity matrix Glutathione Sepharose 4B. Fusion proteins were eluted under mild conditions and gel purified. Cx43 COOH terminus was released from the GST and gel purified again; Cx40-GST was used as a standard directly. The protein content of the gel-purified proteins was determined, and amounts corresponding to 0.5–8 pmol of the Cx protein were
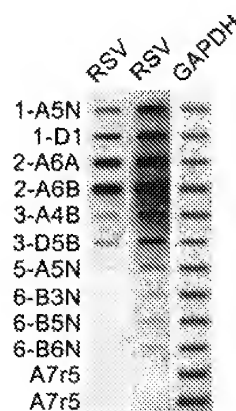

Fig. 2. Slot blot shows RSV (*left lane*, short exposure; *middle lane*, longer exposure) and glyceraldehyde-3-phosphate dehydrogenase (GAPDH; *right lane*) content of pRSV-Cx43AS clones as well as A7r5 controls. Note the low RSV content of the 6B5N clone and the high content of the 2A6 clones.
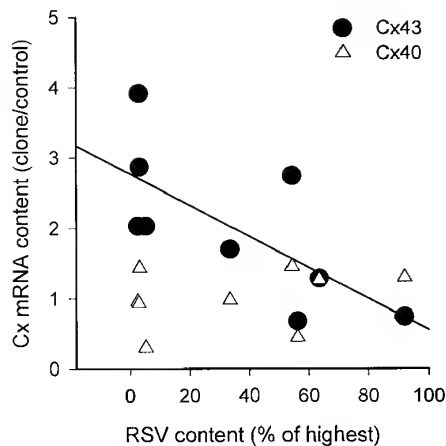
Fig. 3. Cx43 and Cx40 mRNA levels (relative to levels observed in control A7r5 cells) vs. RSV levels in the pRSV-Cx43AS transfectants. Note the inverse relationship between Cx43 mRNA content and RSV content ($r = 0.698$, $P < 0.05$). Cx40 mRNA content was not related to RSV content ($r = 0.28$, $P > > 0.05$).

Table 2. *Cx43 mRNA content of CMV-Cx43AS clones and 6B5N and A7r5 cells*

Clone	n	Cx43
pCMV-AS1	5	$7.6 \pm 1.1*$
pCMV-AS2	5	8.4 ± 3.5
pCMV-AS23	7	$6.3 \pm 1.2*$
6B5N	7	$53.3 \pm 14*$
pRc/CMV-control		11.6 ± 1.0
A7r5	7	10.5 ± 0.84

Cx43 content of total RNA was measured. mRNA values are expressed in arbitrary units following normalization to glyceraldehyde-3-phosphate dehydrogenase (GAPDH) content; n = no. of samples evaluated. Two pCMV vector-only controls were evaluated, once each; the value represents the average of these determinations ± range. *Different from A7r5 at $P \le 0.05$.

loaded either in separate lanes or in a staggered fashion in the same lane. The counts from these standards were used to construct a standard curve against which the connexin content of the samples could be compared.

Dye injections and junctional conductance measurements. The extent of dye coupling was determined as follows. Cells were plated at confluent density (15,000 cells/cm^2) onto glass coverslips. Twenty-four hours after cells were plated, the glass coverslips were mounted in a perfusion chamber and visualized on a microscope equipped with differential interference contrast and fluorescence optics. A microelectrode containing 0.5% Lucifer yellow was lowered onto the surface of a cell, and the cell was impaled by overcompensation of the capacitance compensation feature of the amplifier (WPI 700). The number of cells containing dye was determined 5 min after injection.

Junctional conductance (g_j) was determined by using dual-whole cell voltage-clamp strategies as described previously (20). To minimize the effects of series resistance, we restricted our analysis of g_j to pairs wherein the sum of pipette series resistances was between 20 and 35 MΩ. Under these recording conditions, g_j is underestimated. However, when the series resistances of compared groups do not differ, g_j is underestimated to the same extent in those groups. Any differences in g_j between groups with equal series resistances would remain significant after correction for series resis-
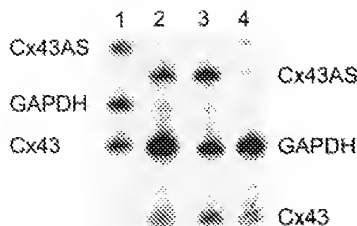
tance. Cells were bathed in a solution containing (in mM) 142.5 NaCl, 4 KCl, 1 MgCl$_2$, 5 glucose, 2 sodium pyruvate, 10 HEPES, 15 CsCl, 10 tetraethylammonium chloride (TEACl), 1 BaCl$_2$, and 1 CaCl$_2$. The patch pipette contained (in mM) 124 KCl, 14 CsCl, 9 HEPES, 9 EGTA, 0.5 CaCl$_2$, 5 glucose, 9 TEACl, 3 MgCl$_2$, and 5 Na$_2$ATP. The pH and osmolarity of both solutions were adjusted to 7.2 and 322 mosM, respectively. Electrodes were fabricated from 1.2-mm glass (Corning 6020, AM Systems) on a Flaming/Brown Micropipette Puller (model P87; Sutter Instruments).

RESULTS

Initially, 17 A7r5 clones and 7 pRSV-Cx43AS clones were isolated, and the mRNA contents of each were quantified by using oligomer probes. The Cx43:Cx40 mRNA ratios for these clones varied as a function of Cx43 content (Fig. 1), suggesting that the level of Cx43 expression largely determined the ratio. The data revealed a fairly broad range of Cx43 content as well as Cx43:Cx40 ratios. The Cx43:Cx40 ratio of the pRSV-Cx43AS clones increased linearly ($r^2 = 0.81$) with Cx43 content. The clone with the highest Cx43:Cx40 ratio, 6B5N, and that with the lowest ratio, 2A6, as well as several isolates of the parental population, were evaluated for expression levels by using both the oligomer

Fig. 4. Cx43AS mRNA was detected by ribonuclease protection assay in 2A6 (*lane 2*) and 6B5N (*lane 3*) cells but not in A7r5 cells (*lane 4*). Interestingly, the 6B5N cells would appear to have more Cx43AS than the 2A6 cells. GAPDH and Cx43 were detected in all samples. *Lane 1* shows nondigested probes.
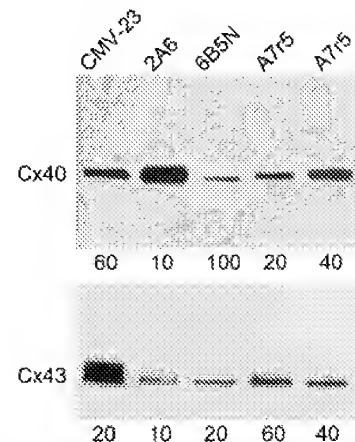

Fig. 5. Western blots of total protein isolated from the indicated cell lines and probed for Cx40 or Cx43 content, as indicated. Protein loading (in μg) is indicated below each lane.

Fig. 6. Western blots of total protein (70 μg/lane) from CMV23 (*lane A*), 6B5N (*lane B*), 2A6 (*lane C*), and A7r5 (*lane D*) cells probed with Cx43 (*A*) or Cx40 antibody (*B*) and visualized with ^{35}S-labeled antirabbit Ig. Cx43- and Cx40-specific bands are labeled; n.s. band represents nonspecific binding of the secondary antibody. Protein standards (*A*: 0.5, 1, 2, and 4 pmol; *B*: 1, 2, 4, and 8 pmol) were loaded in a staggered fashion at ~15-min intervals (*left lane*) in each blot. *C*: counts associated with each of the protein standard bands increase linearly as a function of their protein contents.
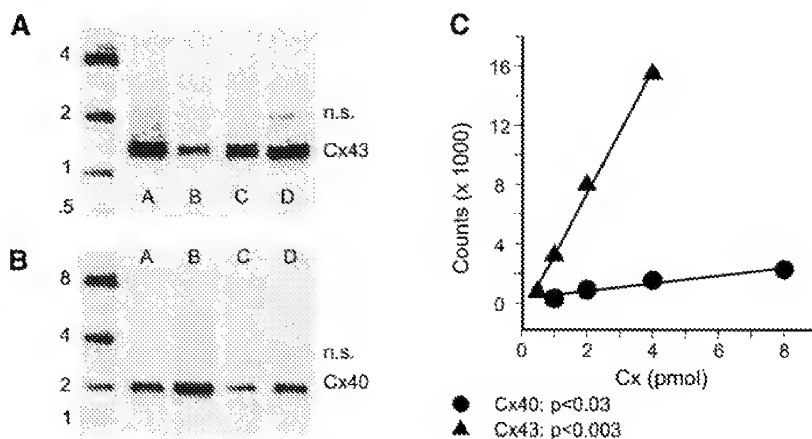
and cDNA probe strategies. Although the absolute values of the results from the two strategies differed (Table 1), both strategies indicated that the Cx43:Cx40 ratio was elevated in the 6B5N vs. A7r5 cells and reduced in the 2A6 vs. A7r5 cells.

Because Cx43 mRNA levels were elevated (relative to the parental A7r5 cells) in several of the antisense Cx43-transfected clones (Fig. 1), we determined whether the Cx43 mRNA content of the antisense-transfected clones was related to the number of copies of the antisense gene stably incorporated into the DNA of the clones. This was accomplished by determining the RSV DNA levels by using a modified Southern analysis as described in MATERIALS AND METHODS. RSV promoter sequence was detected in all of the pRSV-Cx43AS clones but not in nontransfected A7r5 cells (Fig. 2). Cx43 mRNA content of the pRSV-Cx43AS clones was inversely related to their RSV content (Fig. 3). Cx40 mRNA levels of the pRSV-Cx43AS clones were unrelated to their RSV content. These results link low RSV content (Cx43AS content) to enhanced Cx43 mRNA content in most of the pRSV-Cx43AS clones but also indicate that as Cx43AS mRNA levels increased, Cx43 mRNA levels decreased. Furthermore, these results suggest that the 6B5N cells might have significantly less Cx43AS mRNA than the 2A6 cells. To demonstrate that these clones actually express the antisense mRNA and to evaluate relative expression levels, we used RPA to detect the Cx43AS as well as Cx43 and GAPDH sense mRNAs. Figure 4 demonstrates that both 2A6 and 6B5N cells actively express the antisense Cx43 mRNA.

Because complete knockdown of Cx43 was not observed in any of the pRSV-Cx43AS clones, we stably transfected A7r5 cells with the pRcCMV-Cx43AS vector used by Goldberg et al. (15) to significantly reduce Cx43 expression in Rat 1 cells. Using RPA techniques, we found that Cx43 mRNA levels were reduced by 24–43% in three CMV-Cx43AS clones. RPA was also used to verify the elevation of Cx43 mRNA observed by Northern techniques in the 6B5N cells. Consistent with the data presented in Table 1, Cx43 mRNA was

elevated 4.8-fold above that in A7r5 controls in the 6B5N cells (Table 2).

Despite the failure of the antisense Cx43 mRNA in these clones to produce substantial knockdown of sense Cx43 mRNA, the data described indicated that we had successfully isolated stable cell lines with expression ratios differing by approximately fivefold. To determine whether protein levels were well predicted by the mRNA levels, we used Western blots to assay Cx43 and Cx40 levels in total protein isolated from each of these cell lines. Initially, bound antibody was visualized by using HRP-conjugated secondary antibody and enhanced chemiluminescent techniques. A typical blot is shown in Fig. 5. Note that the banding pattern of Cx43 in the 6B5N and 2A6 cells is comparable to that of the parental A7r5 cells, suggesting that phosphorylation of Cx43 was comparable in these cell types. In contrast, the CMV23 cells displayed high levels of the more slowly migrating forms of Cx43, which have been demonstrated by others (18, 19, 21) to be indicative of phosphorylation of the protein and loss of communication.
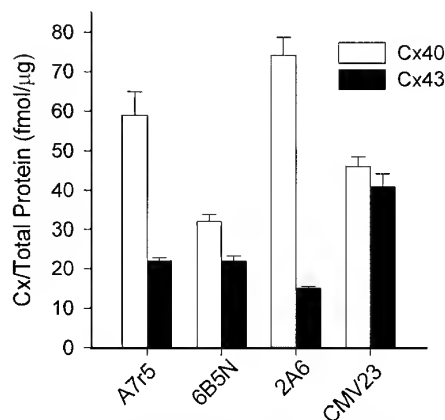

Fig. 7. Cx43 and Cx40 contents of A7r5, 6B5N, 2A6, and CMV23 clones. Cx43 data were derived from 4 sample sets; Cx40 data were derived from 3 sample sets.

Table 3. *Electrical coupling levels in A7r5 parental cells and in 6B5N, 2A6, and CMV23 Cx43AS-transfected clones*

Clone	n	g_j, nS	R_s, MΩ
A7r5	13	33 ± 1.5	25 ± 1.4
6B5N	12	31 ± 1.5	28 ± 1.3
2A6	9	33 ± 3.5	24 ± 1.2
CMV23	5	24 ± 2.4	27 ± 2.2

Values are means ± SE, n = no. of samples. g_j, Junctional conductance; R_s, series resistance.

Quantification of expression ratios using ECL proved difficult because of variability in signal from blot to blot. Therefore, we evaluated Cx40 and Cx43 levels in total protein from 6B5N, 2A6, CMV23, and parental A7r5 cells by using a radioactive secondary antibody and protein standards against which samples could be compared (see MATERIALS AND METHODS). Typical blots for both connexins are shown in Fig. 6. The blots reveal that both the Cx40 and Cx43 contents of the clones differed from that of the parental cells. Relative to the A7r5 parental cells, the 6B5N cells contained less Cx40 and comparable amounts of Cx43, the 2A6 cells contained more Cx40 and less Cx43, and the CMV23 cells contained more of both proteins. The results from multiple samples are summarized in Fig. 7. These connexin contents predict ratios (see Table 1) that differ by more than threefold between the 2A6 and 6B5N cells.

Intercellular communication was characterized in the 6B5N, 2A6, and CMV23 clones and was compared with that in A7r5 parental cells to evaluate whether the change in Cx43:Cx40 ratio and the apparent phosphorylation state of Cx43 influenced communication. g_j was not different among the four cell types ($P > 0.06$, ANOVA), although with a larger sample size it is likely
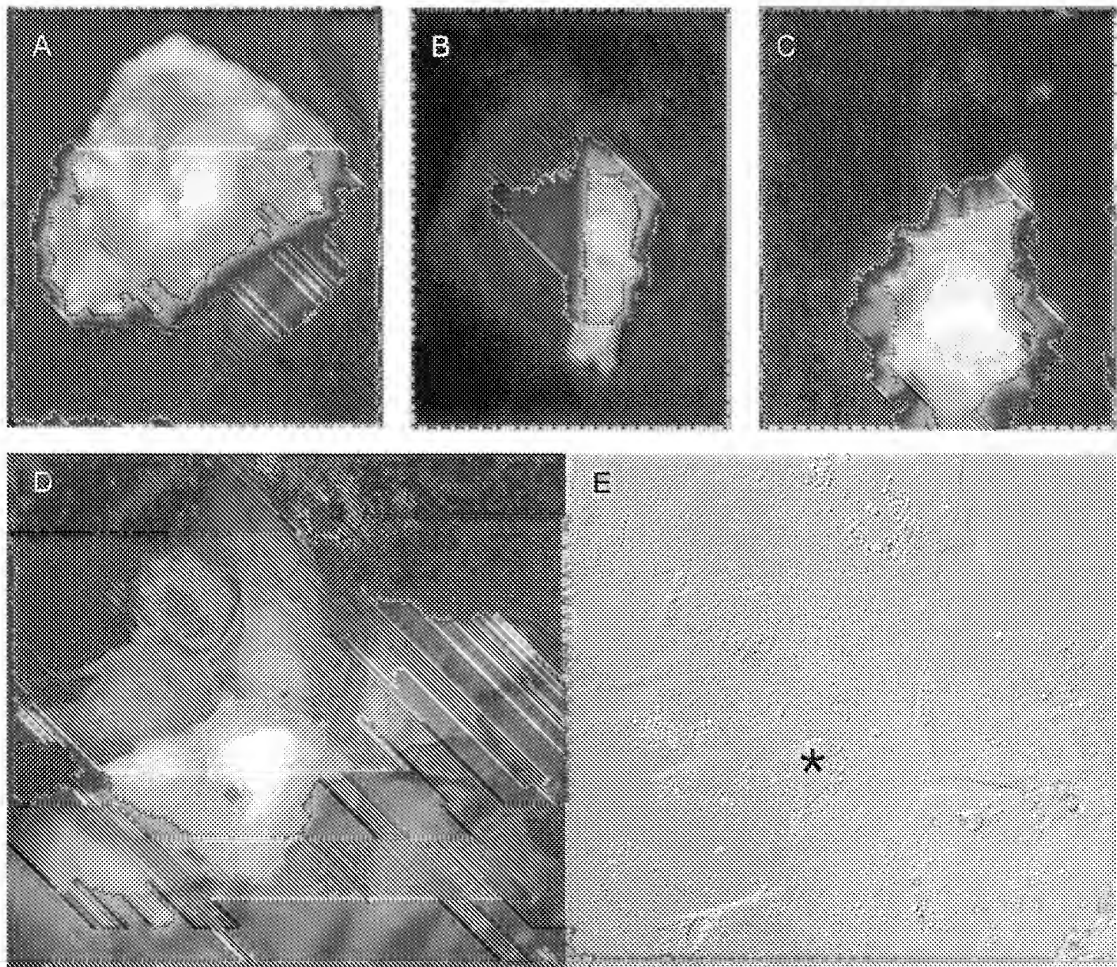

Fig. 8. Lucifer yellow dye coupling was extensive in 6B5N cells (*D* and *E*) compared with that in A7r5 (*A*), CMV23 (*B*), and 2A6 cells (*C*). *A*: 2 neighboring cells contain small amounts of dye. *B* and *C*: low levels of dye were observed in only 1 neighboring cell (electrode observed in bottom of *C*). *D*: the brightest cell was injected; dye was observed in many neighboring cells very quickly after injection (picture at 5 min). *E*: differential interference contrast image of cells in *D* with injected cell marked by asterisk.
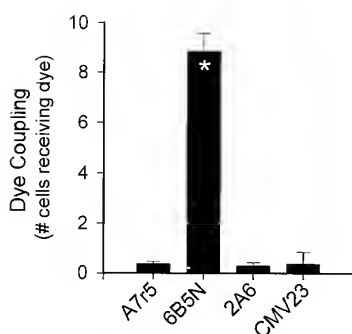
Fig. 9. Dye coupling is significantly enhanced in 6B5N cells (asterisk) compared with A7r5, 2A6, and CMV23 cells. The number of injected cells was as follows: A7r5, 61; 6B5N, 59; 2A6, 20; and CMV23, 21.

that a significant difference would be observed for the CMV23 cells (Table 3). Although g_j is underestimated in these experiments because of the series resistances of the recording electrodes (Table 3), since series resistances were comparable across cell types, g_j is underestimated to the same degree across cell types. Therefore the absence of differences in g_j among cell types is significant.

On the basis of reported differences in Cx40 vs. Cx43 channel selectivity (1, 35), we hypothesized that the permeability of the junctions to large dye molecules would, despite the absence of differences in g_j, be significantly greater in 6B5N than in A7r5 or 2A6 cells. Furthermore, because the appearance of Cx43 in bands that migrate more slowly on SDS-polyacrylamide gels is associated with increased phosphorylation and reduced coupling, we hypothesized that the CMV23 cells, despite their higher Cx43:Cx40 ratio, would also be poorly coupled. To test these hypotheses, we determined the extent of Lucifer yellow dye coupling in these cell lines. Representative dye injections for the four cell types are shown in Fig. 8, and data from multiple injections are summarized in Fig. 9. The 6B5N cells were significantly better dye coupled (Lucifer Yellow) than the other cell types. These data indicate that gap junction permeability was elevated when the Cx43:Cx40 ratio was elevated (6B5N cells); but this enhanced permeability can be compromised by posttranslational modification (e.g., phosphorylation) of the Cx43 protein (CMV23 cells).

DISCUSSION

Recent data indicate that Cx40 and Cx43 form functional heteromeric (17), homomeric/heterotypic (31), and heteromeric/heterotypic channels (Cottrell GT and Burt JM, unpublished observations). Thus as many as 196 channel types (4, 17) are theoretically possible in cells that coexpress these proteins. To understand what the functional consequences of this diversity of channel types might be, clones of a particular cell line that express different ratios of the connexins of interest are needed. The goal of the present study was to
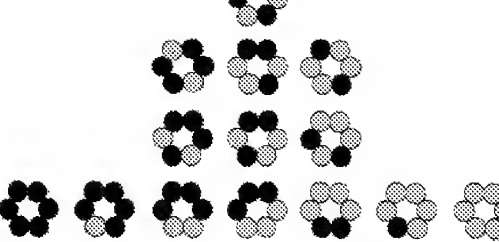
generate A7r5 cell clones that display different Cx43:Cx40 expression ratios and to begin evaluation of whether they display different junctional properties.

Multiple clones of Cx43AS-transfected, vector-only-transfected, and nontransfected A7r5 cells were isolated. These clones displayed a range of Cx43:Cx40 mRNA ratios. In some clones, Cx40 mRNA levels were altered to a far greater extent than Cx43 mRNA levels. However, the changes in Cx40 mRNA levels were unrelated to the efficiency of transfection, which suggests that the variability in Cx40 levels represents spontaneous clonal variation. In general, clones with elevated Cx43:Cx40 mRNA ratio also had elevated Cx43:Cx40 protein ratio; however, the mRNA levels for each connexin were not strictly predictive of the protein levels for the connexins. The failure of mRNA levels to accurately predict protein levels may indicate that connexin gene expression is regulated at multiple levels, transcriptionally as well as posttranscriptionally. The finding that changes in the level of one connexin did not consistently alter expression of the other indicates that expression of these two connexins must be independently regulated.

The significance of altered protein ratios to junctional function appears profound. Although junctional conductance was comparable across cell types, the 6B5N cells were >25 times better dye coupled than the A7r5 cells. Given the similarity of series resistances across cell types, it is highly unlikely that complications arising from series resistance would cause a 25-fold underestimate of g_j in the 6B5N vs. A7r5 cells. Thus the data suggest that the nearly 2-fold difference in Cx43:Cx40 expression ratio in 6B5N vs. A7r5 cells (0.67 vs. 0.37) caused a >25-fold difference in the extent of dye coupling with no change in electrical coupling.

If heteromeric channel assembly is a random process, then the relative contribution of each of the 196 possible channel types to the total pool of channels should reflect the expression ratio of the two connexins.

Table 4. *Predicted connexon frequency for various expression ratios*

Cx43:Cx40	6:0	5:1	4:2	3:3	2:4	1:5	0:6
0.20	<0.01	0.07	0.83	5.5	20.4	40.2	33.0
0.37	0.04	0.63	4.2	15.3	31.1	33.6	15.1
0.67	0.42	3.8	14.0	27.8	31.0	18.4	4.6
0.89	1.1	7.3	20.6	30.9	26.2	11.8	2.2

Assuming random assembly, the probability of forming a specific connexon can be calculated as

$$P_{rCx1:(n-r)Cx2} = (\%Cx_1^r)(\%Cx_2^{n-r})[n!/r!(n-r)!]$$

where $\%Cx_1$ is the percentage of connexin1 in the total pool of connexins, $n = 6$ (connexins in a connexon), and r is the number of subunits of Cx_1 in the heteromer of interest. The probability of forming a specific channel can be calculated as the product of the two connexon probabilities. Assuming random assembly, probability theory predicts that an increase in Cx43:Cx40 expression ratio from 0.37 to 0.67 (A7r5 vs. 6B5N) would result in an ~118-fold increase in homomeric/homotypic Cx43 channels and a 14-fold increase in the channel population wherein both connexons contain four or more Cx43 subunits (see Table 4). We do not know the connexin composition of the channel types that mediate the bulk of the dye permeation observed in our studies. Homomeric/homotypic Cx40 channels appear to be highly cation selective, whereas Cx43 channels are reasonably well permeated by ions of both charges as well as by large fluorescent dyes. The permeation properties of Cx40/43 heterotypic and heteromeric channels are unknown. However, published data indicate that the behavior of such channels is not readily predicted by the behavior of the homomeric/homotypic channels. He et al. (17), Valiunas et al. (31), and Cottrell and Burt (unpublished work) have demonstrated that single-channel amplitudes and voltage-dependent gating were significantly different in the heterotypic and heteromeric settings relative to the homomeric/homotypic setting, suggesting that heteromeric channels may exhibit different selectivities and gating properties. Probability theory predicts that small changes in expression ratio could significantly alter the connexin composition of the channel population. Our data suggest that changes in expression ratio profoundly influence gap junction selectivity.

If such changes in expression ratio were to occur in vivo during development (11, 33) or as a consequence of disease, injury, or disturbed flow (13, 14, 27, 28, 32), then our data suggest that electrical signaling could be preserved while intercellular exchange of metabolites and large second messenger signaling molecules would be greatly altered. In cells that rely on electrical signals to coordinate their activity, such as the heart and blood vessels, the capacity to maintain electrical signaling while dramatically altering the exchange of other types of signaling molecules could be of considerable importance to organ function and animal survival. Kurjiaka et al. (20) demonstrated that A7r5 cells maintained in 1% vs. 10% serum were significantly better dye coupled despite comparable levels of electrical coupling. The present data suggest that this enhanced dye coupling could result from an increase in the Cx43:Cx40 expression ratio in the growth-arrested cells.

In summary, we have generated several cell lines that express a range of Cx43:Cx40 protein ratios. The data from these cell lines suggest that junctional permeability can be regulated not only through phosphor-ylation of channel proteins but also through alteration of the connexin composition of heteromeric channels. The latter strategy would likely occur over a longer time course, comparable to protein turnover rates, and is thus complementary to the phosphorylation strategy.

REFERENCES

1. **Beblo DA and Veenstra RD.** Monovalent cation permeation through the connexin40 gap junction channel Cs, Rb, K, Na, Li, TEA, TMA, TBA, and effects of anions Br, Cl, F, acetate, aspartate, glutamate, and NO_3. *J Gen Physiol* 109: 509–522, 1997.
2. **Beyer EC, Reed KE, Westphale EM, Kanter HL, and Larson DM.** Molecular cloning and expression of rat connexin40, a gap junction protein expressed in vascular smooth muscle. *J Membr Biol* 127: 69–76, 1992.
3. **Blackburn JP, Peters NS, Yeh HI, Rothery S, Green CR, and Severs NJ.** Upregulation of connexin43 gap junctions during early stages of human coronary atherosclerosis. *Arterioscler Thromb Vasc Biol* 15: 1219–1228, 1995.
4. **Brink PR, Cronin K, Banach K, Peterson E, Westphale EM, Seul KH, Ramanan SV, and Beyer EC.** Evidence for heteromeric gap junction channels formed from rat connexin43 and human connexin37. *Am J Physiol Cell Physiol* 273: C1386–C1396, 1997.
5. **Bruzzone R, Haefliger JA, Gimlich RL, and Paul DL.** Connexin40, a component of gap junctions in vascular endothelium, is restricted in its ability to interact with other connexins. *Mol Biol Cell* 4: 7–20, 1993.
6. **Bruzzone R, White TW, and Paul DL.** Connections with connexins: the molecular basis of direct intercellular signaling. *Eur J Biochem* 238: 1–27, 1996.
7. **Bukauskas FF, Elfgang C, Willecke K, and Weingart R.** Biophysical properties of gap junction channels formed by mouse connexin40 in induced pairs of transfected human HeLa cells. *Biophys J* 68: 2289–2298, 1995.
8. **Campos de Carvalho AC, Roy C, Moreno AP, Melman A, Hertzberg EL, Christ GJ, and Spray DC.** Gap junction formed of connexin43 are found between smooth muscle cells of human corpus cavernosum. *J Urol* 49: 1568–1575, 1993.
9. **Christ GJ, Spray DC, El-Sabban ME, Moore LK, and Brink PR.** Gap junctions in vascular tissues: role of heterotypic and homotypic intercellular communication in the modulation of vasomotor tone. *Circ Res* 79: 631–646, 1996.
11. **Delorme B, Dahl E, Jarry-Guichard T, Briand JP, Willecke K, Gros D, and Theveniau-Ruissy M.** Expression pattern of connexin gene products at the early developmental stages of the mouse cardiovascular system. *Circ Res* 81: 423–437, 1997.
12. **Elfgang C, Eckert R, Lichtenberg-Frate H, Butterweck A, Traub O, Klein RA, Hulser D, and Willecke K.** Specific permeability and selective formation of gap junction channels in connexin-transfected HeLa cells. *J Cell Biol* 129: 805–817, 1995.
13. **Elvan A, Huang XD, Pressler ML, and Zipes DP.** Radiofrequency catheter ablation of the atria eliminates pacing-induced sustained atrial fibrillation and reduces connexin 43 in dogs. *Circulation* 96: 1675–1685, 1997.
14. **Gabriels JE and Paul DL.** Connexin43 is highly localized to sites of disturbed flow in rat aortic endothelium but connexin37 and connexin40 are more uniformly distributed. *Circ Res* 83: 636–643, 1998.
15. **Goldberg GS, Martyn KD, and Lau AF.** A connexin 43 antisense vector reduces the ability of normal cells to inhibit the foci formation of transformed cells. *Mol Carcinog* 11: 106–114, 1994.
16. **Gu H, Ek-Vitorin JF, Taffet SM, and Delmar M.** Co-expression of connexins 40 and 43 enhances the pH sensitivity of gap junctions. A model for synergistic interactions among connexins. *Circ Res* 86: e98-e103, 2000.

17. He DS, Jiang JX, Taffet S, and Burt JM. Formation of heteromeric gap junction channels by connexins 40 and 43 in vascular smooth muscle cells. *Proc Natl Acad Sci USA* 96: 6495–6500, 1999.

18. Hossain MZ, Ao P, and Boynton AL. Platelet-derived growth factor-induced disruption of gap junctional communication and phosphorylation of connexin43 involves protein kinase C and mitogen-activated protein kinase. *J Cell Physiol* 176: 332–341, 1998.

19. Kanemitsu MY and Lau AF. Epidermal growth factor stimulates the disruption of gap junctional communication and connexin43 phosphorylation independent of 12-O-tetradecanoylphorbol 13-acetate-sensitive protein kinase C: the possible involvement of mitogen-activating protein kinase. *Mol Biol Cell* 4: 837–848, 1993.

20. Kurjiaka DT, Steele TD, Olsen MV, and Burt JM. Gap junction permeability is diminished in proliferating vascular smooth muscle cells. *Am J Physiol Cell Physiol* 275: C1674–C1682, 1998.

21. Lau AF, Kanemitsu MY, Kurata WE, Danesh S, and Boynton AL. Epidermal growth factor disrupts gap junctional communication and induces phosphorylation of Connexin43 on serine. *Mol Biol Cell* 3: 865–874, 1992.

22. Little TL, Beyer EC, and Duling BR. Connexin43 and connexin40 gap junctional proteins are present in both arteriolar smooth muscle and endothelium in vivo. *Am J Physiol Heart Circ Physiol* 268: H729–H739, 1995.

23. Moore LK, Beyer EC, and Burt JM. Characterization of gap junction channels in A7r5 vascular smooth muscle cells. *Am J Physiol Cell Physiol* 260: C975–C981, 1991.

24. Moore LK and Burt JM. Selective block of gap junction channel expression with connexin-specific antisense oligodeoxynucleotides. *Am J Physiol Cell Physiol* 267: C1371–C1380, 1994.

25. Moore LK and Burt JM. Gap junction function in vascular smooth muscle: influence of serotonin. *Am J Physiol Heart Circ Physiol* 269: H1481–H1489, 1995.

26. Moreno AP, Saez JC, Fishman GI, and Spray DC. Human Connexin43 gap junction channels: regulation of unitary conductances by phosphorylation. *Circ Res* 74: 1050–1057, 1994.

27. Peters NS. New insights into myocardial arrhythmogenesis: distribution of gap-junctional coupling in normal, ischaemic and hypertrophied human hearts - Glaxo/MRS Young Investigator Prize. *Clin Sci (Colch)* 90: 447–452, 1996.

28. Peters NS, Coromilas J, Severs NJ, and Wit AL. Disturbed connexin43 gap junction distribution correlates with the location of reentrant circuits in the epicardial border zone of healing canine infarcts that cause ventricular tachycardia. *Circulation* 95: 988–996, 1997.

29. Rennick RE, Connat JL, Burnstock G, Rothery S, Severs NJ, and Green CR. Expression of connexin43 gap junctions between cultured vascular smooth muscle cells is dependent upon phenotype. *Cell Tissue Res* 271: 323–332, 1993.

30. Sambrook J, Fritsch EF, and Maniatis T. *Molecular Cloning*. Plainview, NY: Cold Spring Harbor, 1989.

31. Valiunas V, Weingart R, and Brink PR. Formation of heterotypic gap junction channels by connexins 40 and 43. *Circ Res* 86: e42–e49, 2000.

32. Van der Velden HM, Van Kempen MJ, Wijffels MC, van Zijverden M, Groenewegen WA, Allessie MA, and Jongsma HJ. Altered pattern of connexin40 distribution in persistent atrial fibrillation in the goat. *J Cardiovasc Electrophysiol* 9: 596–607, 1998.

33. Van Kempen MJ, Vermeulen JL, Moorman AF, Gros D, Paul DL, and Lamers WH. Developmental changes of connexin40 and connexin43 mRNA distribution patterns in the rat heart. *Cardiovasc Res* 32: 886–900, 1996.

34. Veenstra RD, Wang HZ, Beblo DA, Chilton MG, Harris AL, Beyer EC, and Brink PR. Selectivity of connexin-specific gap junctions does not correlate with channel conductance. *Circ Res* 77: 1156–1165, 1995.

35. Wang HZ and Veenstra RD. Monovalent ion selectivity sequences of the rat connexin43 gap junction channel. *J Gen Physiol* 109: 491–507, 1997.

36. White TW, Paul DL, Goodenough DA, and Bruzzone R. Functional analysis of selective interactions among rodent connexins. *Mol Biol Cell* 6: 459–470, 1995.